



Study of surface modification of nano-SiO₂ with macromolecular coupling agent (LMPB-g-MAH)

Yanlong Tai^{a,b}, Jiasheng Qian^{a,b,*}, Yuchuan Zhang^{a,b}, Jinde Huang^{a,b}

^a Chemical Engineering, Anhui University, PR China

^b The Key Laboratory of Environment-friendly Polymer materials of Anhui Province, School of Chemistry, Feixi Road, Hefei, Anhui, 230039, PR China

ARTICLE INFO

Article history:

Received 19 November 2007
Received in revised form 1 March 2008
Accepted 4 March 2008

Keywords:

Macromolecular coupling agent
Silicon dioxide nano-particles
Surface modified
Using efficiency

ABSTRACT

Commercial silicon dioxide nano-particles were modified by graft copolymerization macromolecular coupling agents (LMPB-g-MAH) of maleic anhydride (MAH) onto low-molecular-weight polybutadiene liquid rubber (LMPB) in dimethylbenzene. The hydroxyl groups on the surface of nano-SiO₂ particles can interact with anhydride groups [-(C=O)₂-O-] of LMPB-g-MAH and an organic coating layer was formed. The covalent bands [-(C=O)-O-, -(C=O)-NH-] formed was testified by Fourier transform infrared spectra (FT-IR). Through transmission electron micrograph (TEM) observation, it was found that LMPB-g-MAH improved the dispersibility of nano-SiO₂ particles in dimethylbenzene. By using the particle size analysis, it was confirmed that the optimum graft degree (GD%) and the optimum loading of LMPB-g-MAH is 9–11%, 10–12%, respectively. The dispersion stabilization of modified SiO₂ nano-particles in dimethylbenzene was significantly improved due to the introduction of grafted polymers on the surface of nano-particles. Thermo gravimetric analysis (TGA) and contact angle measurement indicated that LMPB-g-MAH molecules were absorbed or anchored on the surface of nano-SiO₂ particle and the using efficiency is 74.66%, which facilitated to hinder the aggregation of nano-SiO₂ particles.

© 2008 Elsevier B.V. All rights reserved.

1. Introduction

In recent years, much research attention has been paid to nano-particles, which possess novel optical, electronic and chemical properties absent in bulk materials. Silicon dioxide (SiO₂) is one of the most important materials for many fields such as chemical sensors, varistors, thin film photovoltaic solar cells, piezoelectric and luminescent devices, catalysts and cosmetic materials [1–5]. But nano-particles have a strong tendency to agglomerate due to its high surface energy, and have weak combination with the polymer matrix because of badly consistent interface [6–9]. So the surface modification of nano-particles is a very difficult task. The crux lies in the fact how to well disperse inorganic nano-particles in organic polymer matrices and how to improve their interfacial interaction. This has been the critical procedure to prepare high-performance nanocomposites.

Now, there are several methods to modify the surface of silicon dioxide in literatures. Fendler and coworkers [10] modified silicon nanocrystallites with alcohols (1-undecanol, 1-hexadecanol, 1-octanol) to improve the Photoluminescence (PL). Swihart and coworkers [11,12] grafted octadecyltri methoxy silane, octadecene

or undecylenic acid on to the surface of silicon nano-particles, and TEM, FT-IR (Fourier transform infrared spectra), Photoluminescence measurements, etc. were used to describe the results. Ulman [13] reported that long-chain *n*-alkanoic acids (C_nH_{2n+1} + 1COOH) were grafted on the surface of metal and non-metallic oxides by self-assembled monolayers (SAMs). Kang and coworkers [14], used Covalent Graft Polymerization and Block Copolymerization to modify the chlorinated SiO₂ (SiO₂-Cl) by Atom transfer radical polymerization (ATRP).

In our previous work, a series of molecular coupling agent, such as tercopolymer BA-MAA-AN [15], tercopolymer BA-MMA-VTES [16], tercopolymer BA-MMA-GMA [17], etc., was synthesized to modify nano-particles, which was applied to prepare nano-particles/rubber composites. Due to the strong interface action, this nanocomposite we prepared exhibit unique hybrid properties including good heat-resistance, good wear-resistance and good dynamic mechanical properties. It can be guessed that the organic coating layer on the nano-particles modified by macromolecular coupling agent is thicker than small molecular coupling agent, and it can bring more strong electrostatic and steric stabilization. The dispersion sketch of the modified nano-particles in the polymer matrix is showed in Fig. 1 [15–19].

In the study, for nano-SiO₂ particles/weak polarity rubber composite, a new macromolecular coupling agent (LMPB-g-MAH) was designed and synthesized in dimethylbenzene system using

* Corresponding author. Tel.: +86 551 5108643; fax: +86 551 5108643.
E-mail address: qjsh@ahu.edu.cn (J. Qian).

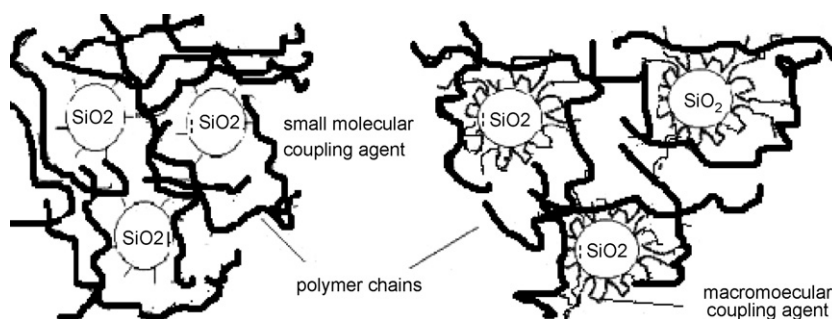


Fig. 1. Schematic drawing of the possible structure of modified nano-SiO₂ dispersed in polymer matrix (a) modified with small molecular coupling agent and (b) modified with macromolecular coupling agent.

benzoyl peroxide (BPO) as initiator [20–23]. On the one hand, maleic anhydride (MAH) as the side group [-(C=O)₂-O-] on the main chain of LMPB-g-MAH may react with -OH which are on the surface of nano-SiO₂ particles containing active hydrogen. On the other hand, low-molecular-weight polybutadiene liquid rubber (LMPB) has the quite similar structure or polarity with BR, NR, NBR, etc., and provides them great compatibility. So, when the macromolecular coupling agent bridged nano-SiO₂ particles with rubber matrix, the entanglements between the long-chains of LMPB-g-MAH and the main rubber matrix will substantially enhance the interactions. Beside the chains of LMPB are full of unsaturated double bonds which can improve the rubber sulfidation.

The dispersion of nano-SiO₂ particles as well as the mechanism of stable colloidal dispersion was discussed in dimethylbenzene [24–26], whose polar is quite low. The using efficiency of LMPB-g-MAH as a modifier was also studied.

2. Experimental

2.1. Materials

Low-molecular-weight polybutadiene liquid rubber was purchased from Beijing Yanshang Petrification Co., Ltd. and the numerical average molecular weight was $M_n = 1000 (\pm 50)$, the content of ethylene is 60–70%, and viscosity is 150–2000 cP (20 °C). MAH (Shanghai Chemical Solvent Factory) were used without further purification. Benzoyl peroxide was purified by recrystallization from acetone. Acetamide was got from Sinopharm Chemical Reagent Co., Ltd. Dimethylbenzene was purified by distillation under nitrogen at reduced pressure before use. Silicon dioxide used for this study was a commercial ultrafine amorphous powder (Hefei Kiln Nanometer Technology Inc., China,) with the following characteristics: average particle diameter 15 nm, specific surface area 115 m² g⁻¹. Other reagents were of analytical grade and used as received.

2.2. Synthesis and purification of LMPB-g-MAH

A 250 ml three necked round-bottomed flask, filled with a stirrer in a temperature-controlled water-bath, was used for the reaction. 10 g of LMPB, 1 g (or 2.5 g, 3.5 g, 4.5 g, 6 g) of MAH and 120 ml of dimethylbenzene were mixed with constantly stirring and bubbling of a slow stream of nitrogen gas for about 30 min at 90 °C. 1 wt% of m_{sample} ($m_{\text{LMPB}} + m_{\text{MAH}}$) of BPO and 30 wt% of m_{BPO} of acetamide dissolved in 30 ml dimethylbenzene, which were slowly added into the flask to initiate the graft polymerization. After 2 h (or 2 h, 2 h.5 h, 3 h, 4 h), the reaction was stopped by letting air into the reactor and cooling the flask. The products, which were called

1#, 2#, 3#, 4#, 5# in turn, were precipitated by pouring the reaction mixture into an alcohol/water mixture. The precipitate was filtered, washed thoroughly with acetone, alcohol, and alcohol/water mixture, alternatively, then vacuum drying at 60 °C for 10 h [27,28].

2.3. Surface modification of nano-SiO₂

The native nano-SiO₂ particles about 3 g were dispersed in 50 ml dimethylbenzene, and a certain amount of LMPB-g-MAH (5 wt%, 7 wt%, 9 wt%, 11 wt%, 13 wt% of nano-SiO₂) was added into the flask, mixing round with high speed at 60 °C for 3.5 h, then vacuum drying for 10 h.

2.4. Instrumental analysis

Fourier transform infrared spectra of LMPB-g-MAH were carried out on spectrometer (Nicolet Co., Nexus-870, USA) with a resolution of 4 cm⁻¹ for which the samples were palletized with KBr powder. The morphology analysis was performed on transmission electron micrograph (TEM) analyzer (Jeol 100CX-II JAPAN). The mean size and size distribution of nano-particles was determined by particle Size Distributions Analyzer (3000HS, Malvern, England). The contact angle and surface free energy were investigated using contact angle measuring instrument (KRUSS GmbH DSA 10-MK2, Germany) at the temperature of 25 °C. Methanol and water were dropped on the sample surface at ten different sites separately. The average values for a sample were taken as its contact angle. The content of intercalated polymer was determined by thermal gravimetric analysis (TGA) on thermal analyzer (Netzsch Co., TG 209, Germany). Samples were heated to 700 °C from room temperature at the speed of 30 °C min⁻¹.

2.5. Measurement of the graft degree (GD%) of LMPB-g-MAH

The GD% of LMPB-g-MAH was determined by a back-titration procedure. 0.5 g purified product was dissolved in dimethylbenzene (about 100 ml) at the boiling temperature for 1 h, then 25 ml 0.05 mol l⁻¹ ethanol solution of NaOH was added, and kept refluxing for 2 h. And then back-titration was performed by 0.01 mol l⁻¹ *iso*-propylalcohol solution of HCl with methyl red as indicator. The acid number and the GD% were calculated according to the following formula [21,27]:

$$GD\% = \frac{N_{\text{NaOH}} \times V_{\text{NaOH}} - N_{\text{HCl}} \times \Delta V_{\text{HCl}}}{2 \times M_{\text{sample}}} \times 98.06 \times 100 \quad (1)$$

where V_{NaOH} (ml): the initial volume of *iso*-propylalcohol solution of NaOH in sample mixture solution; V_{HCl} (ml): the consumption with *iso*-propylalcohol solution of HCl by NaOH in the mixture solution; M_{sample} (g): the weight of LMPB-g-MAH.

Table 1
Different GD% of the macromolecular coupling agents (LMPB-g-MAH)

	1 [#]	2 [#]	3 [#]	4 [#]	5 [#]
GD%	2.36	6.24	10.29	13.11	17.15

2.6. The dispersion stability of nano-SiO₂ particle in dimethylbenzene

The separation of the free LMPB-g-MAH from the LMPB-g-MAH anchored to nano-SiO₂ particles was achieved by dialysis. Typically, 100 ml dimethylbenzene dispersion of 0.1 g modified nano-SiO₂ particles was allowed to stand at room temperature. After a definite time, 5.0 ml of dispersion liquid was taken out with a pipette, and the content of nano-SiO₂ particles dispersed was determined. The stability of dispersion was estimated from percentage of dispersed nano-SiO₂ particles after standing by the following equation [25]:

$$\text{Nano-SiO}_2 \text{ particles dispersed (\%)} = \frac{G}{G_0} \times 100 \quad (2)$$

where G (g) and G_0 (g) are the weight of nano-SiO₂ dispersed after and before standing, respectively.

3. Results and discussion

3.1. Measurement of the GD% of LMPB-g-MAH

Different GD% of macromolecular coupling agents (LMPB-g-MAH) were synthesized in dimethylbenzene using benzoyl peroxide as initiator and acetamide as anti-gelling agent, via the change of the amount of MAH, LMPB, reaction time and reaction temperature. The products were called 1[#], 2[#], 3[#], 4[#], 5[#] by GD% in turn, which can be seen in Table 1.

3.2. FT-IR analysis

It can be seen from Fig. 2(a) that from LMPB-g-MAH 1[#]–5[#], the 1780 cm⁻¹, 1830 cm⁻¹ (C=O stretching vibration mode) and 1310–1210 cm⁻¹ (C–O stretching vibration mode) absorption peaks emerge and are gradually strengthened, while low-molecular-weight polybutadiene liquid rubber do not have the peaks from curve (LMPB), and they are the characteristic peaks of MAH from curve (MAH). So it can be inferred that different quantity of MAH has been grafted onto the macromolecular chains of LMPB [27].

Fig. 2(b) shows typical FT-IR spectra of native nano-SiO₂ particles and the modified nano-SiO₂ particles with LMPB-g-MAH, respectively. From the FT-IR spectra of unmodified nano-SiO₂, we can see that the peak at 3422 cm⁻¹ is attributed to O–H stretching mode, shear vibration near 1630 cm⁻¹, bending mode near 1390 cm⁻¹. The peak at 1103 cm⁻¹ corresponding to the Si–O–Si absorption bands, the asymmetric stretching vibration near 810 cm⁻¹, bending vibration near 487 cm⁻¹ [29].

From the FT-IR spectra of modified nano-SiO₂, the absorption peaks in the region 3000–3300 cm⁻¹ and 2800–3000 cm⁻¹ correspond to the Ar–H, C–H(–C=C–H) and –CH₂–, –CH₃ groups of LMPB-g-MAH, respectively. The strong absorption peak at 1735 cm⁻¹ belongs to C=O (stretching vibration mode) of LMPB-g-MAH. Compared with the absorption bands of [–(C=O)₂–O–] of LMPB-g-MAH at 1780 cm⁻¹ (C=O), 1830 cm⁻¹ (C=O), the shift of absorption band is possible due to the interaction of [–(C=O)₂–O–] with Si–OH groups to form poly(LMPB-g-MAH-SiO₂) complex on the surface of nano-SiO₂.

what's more, the Si–O–Si absorption bands are observed at 1150–1050 cm⁻¹, these are overlapped by Si–O–C absorption (800–1150 cm⁻¹), and thus could not be confirmed by the Si–O–C and Si–O–Si absorption area, but it can be found that the peak of modified nano-SiO₂ particles at 800–1150 cm⁻¹ is broader and stronger than that of the native nano-SiO₂ particles. This indicates that the surface group of nano-SiO₂ has changed from Si–OH to Si–O–C. This proves that the macromolecular coupling agents are tightly absorbed at the surface of nano-SiO₂ by chemisorption, which are still existed on the surface of the modified particles even after being extracted by Soxhlets extractor among dimethylbenzene [30,1].

So, a simple schematic representation of the one-step procedure for attaching an invertible macromolecular coupling agent (LMPB-g-MAH) to a nano-SiO₂ particle surface is shown in Fig. 3 [31].

3.3. TEM morphology of nano-SiO₂ particle

Fig. 4 displays the TEM images of native nano-SiO₂ and modified nano-SiO₂ suspensions in dimethylbenzene. In order to represent detailed morphological information of the specimens, different magnifications are utilized for various samples. The obvious agglomeration can be seen in the images of native nano-SiO₂ (Fig. 4(a)) and the homogeneous dispersion can be seen in the images of modified nano-SiO₂ (Fig. 4(b)). From Fig. 4(b₂), the macromolecular coupling agent (LMPB-g-MAH) layers coated on

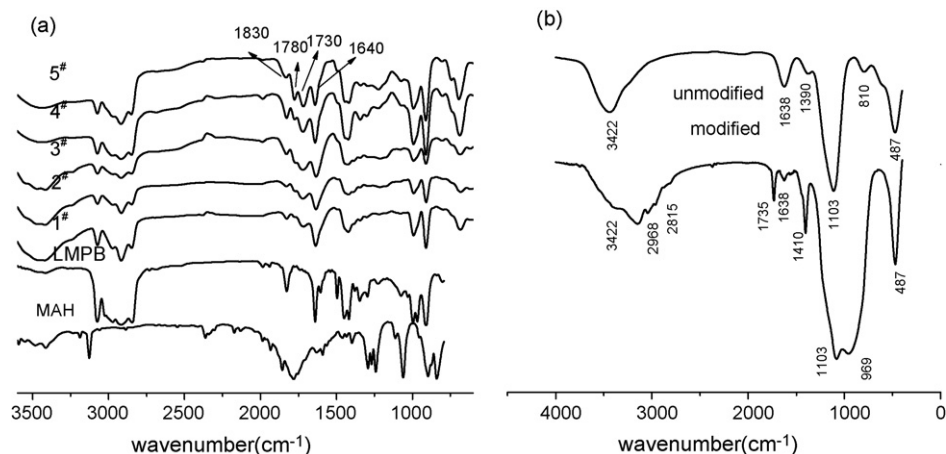


Fig. 2. IR spectra of (a) different GD% of LMPB-g-MAH: (1[#], 2[#], 3[#], 4[#], 5[#]), LMPB, MAH and (b) unmodified nano-SiO₂; modified nano-SiO₂ and extracting.

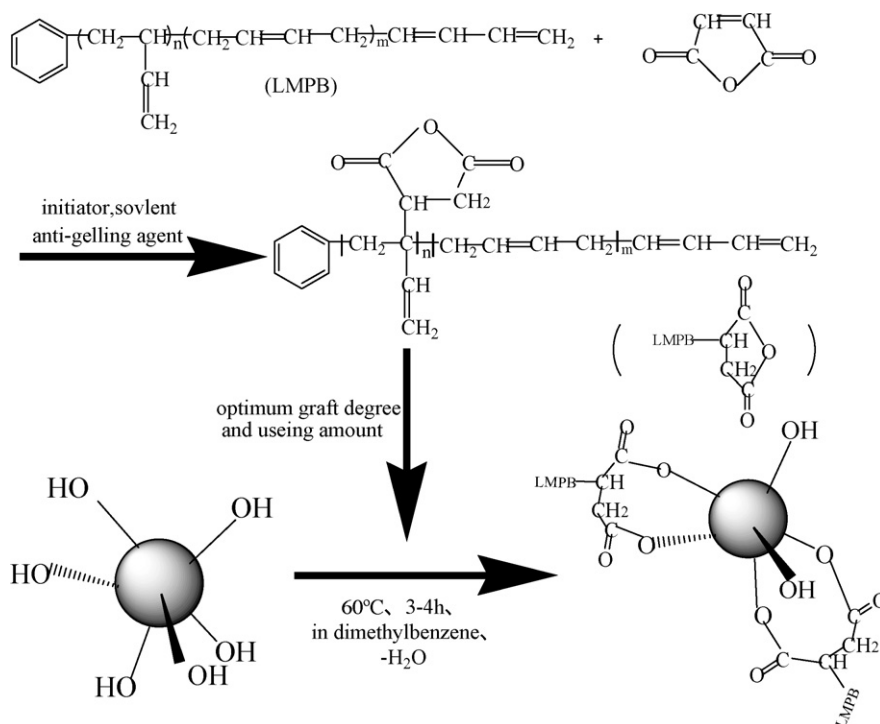


Fig. 3. Schematic representation for the modification of nano-size silicon dioxide particles (SiO₂) with a new macromolecular coupling agent (LMPB-g-MAH).

the surface of nano-SiO₂ particles are clearly shown as the gray area, and the agglomerations has been reduced. This suggests that physical bonding or chemical bonding occurs between the polarity bond of LMPB-g-MAH and hydroxide group, unsaturated bond or suspension bond. The macromolecular chains grafted on the surface of nano-SiO₂ bring mutual exclusion and steric hindrance effect, thus the surface free energy has been reduced correspondingly and the agglomeration controlled. All the results above further illustrate that LMPB-g-MAH has played an important role in the dispersion of nano-SiO₂ particles.

3.4. The stability of nano-SiO₂ particle dispersion in dimethylbenzene

The dispersion stability of modified nano-SiO₂ particles in dimethylbenzene is compared with native nano-SiO₂ particles as shown in Fig. 5. Native nano-SiO₂ particles have been completely precipitated. It can be seen that native SiO₂ nano-particles have been completely precipitated for about 3 days, while the modified SiO₂ nano-particle modified with 3[#] (LMPB-g-MAH) have a stable colloidal dispersion in dimethylbenzene.

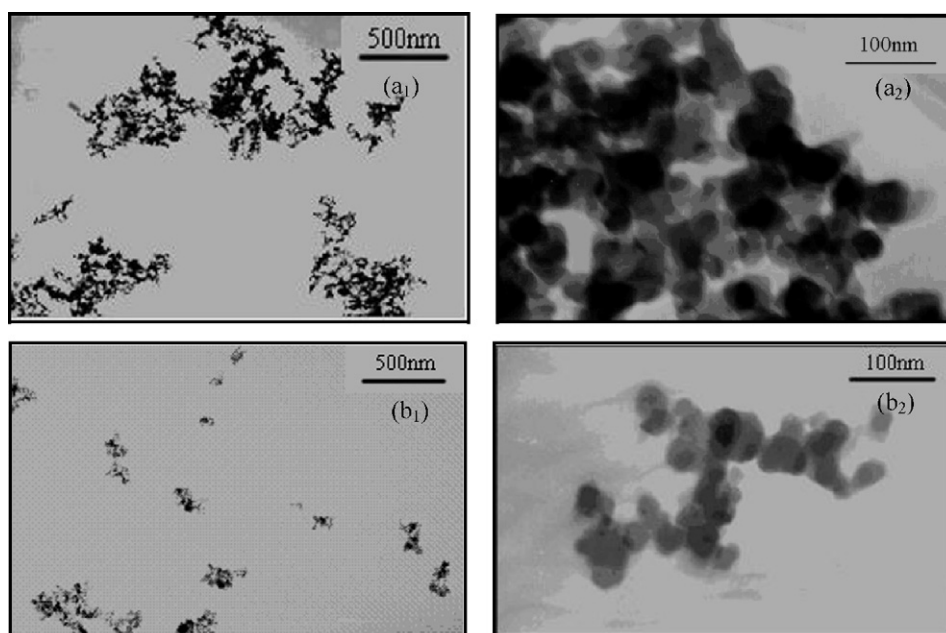


Fig. 4. TEM images for nano-SiO₂: (a) untreated particles and (b) modified with LMPB-g-MAH.

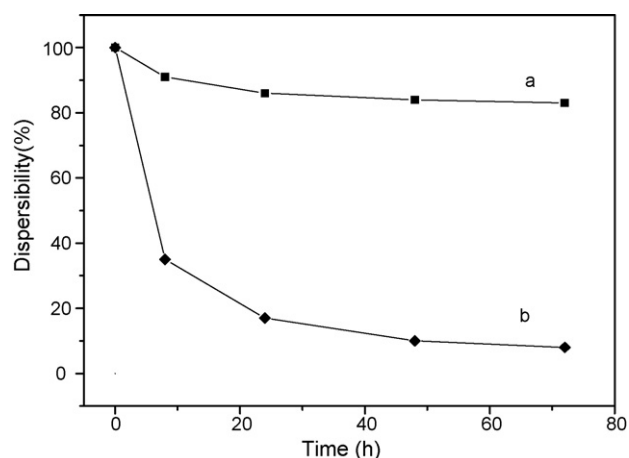


Fig. 5. Stability of nano-SiO₂ particles dispersion in dimethylbenzene: (a) unmodified and (b) modified with 3[#] (LMPB-g-MAH).

The hydroxyl groups (–OH) from nano-SiO₂ particles can interacted with maleic anhydride groups [–(C=O)₂–O–] from LMPB-g-MAH to form (LMPB-g-MAH-g-SiO₂) complex on the surface of nano-SiO₂ particles. Consequently, no matter what reaction occurred, the graft copolymers are initially grafted or anchored on the surface of the particles at one or several spots. The other terminal of LMPB-g-MAH is organic polymer chain, which fulfills steric hindrance between inorganic nano-particles. All above factors give rise to the homogeneous dispersion of SiO₂ nano-particles in dimethylbenzene and maintain a stable colloidal dispersion for a long time. We can more intuitionistic see from Fig. 6. They are the photographs of dispersion stabilized of nano-SiO₂ in dimethylbenzene by time.

3.5. Analysis of SiO₂ nano-particle size and distribution

The nano-SiO₂ suspension in dimethylbenzene is prepared by the ultrasonic vibrating method. On the basis of dynamic light scattering (DLS) principle, the number average diameter and size distribution of nano-SiO₂ suspension is analyzed using Size Distributions Analyzer (as shown in Figs. 7 and 8 and Tables 2 and 3). The native nano-SiO₂ particles are dispersed poorly in dimethylbenzene and the serious agglomerations are formed due to the existence of Si–OH groups. Compared with the native particles, nano-SiO₂ modified with LMPB-g-MAH shows good dispersion in dimethylbenzene. Because of the new chemical bond's form between macromolecular coupling agent and nano-particles, the interaction among nano-particles is broken down and the agglomeration controlled effectively. According to the result, the average diameter of native nano-SiO₂ is about 700–900 nm while that of modified nano-SiO₂ decreases obviously.

Table 2
Average diameter and size distribution of nano-SiO₂ (by number)

Coupling agent (#)	0%	1 [#]	2 [#]	3 [#]	4 [#]	5 [#]
Average diameter (nm)	810.8	169	108.6	41.7	56.1	46.8
Size distribution (nm)	550–1250	145–205	46–400	28–65	25–200	26–100

Table 3
Average diameter and size distribution of nano-SiO₂ (by number)

Coupling agent (%)	0%	5%	7%	9%	11%	13%
Average diameter (nm)	810.8	64.7	92.1	35.9	41.7	109.0
Size distribution (nm)	550–1250	45–450	45–400	20–100	28–65	70–155

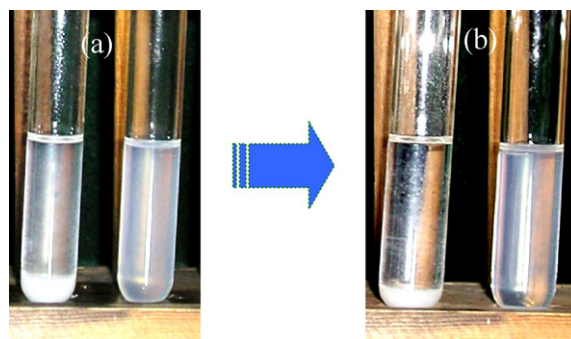


Fig. 6. Photographs of dispersion stabilized of nano-size silicon dioxide particles (SiO₂) in polybutadiene solution by time: (a) ultrasonic dispersion samples after 10min and (b) ultrasonic dispersion samples after 3 days, and the left is unmodified silicon dioxide sample, the right is modified silicon dioxide sample.

Fig. 7 shows, with the GD% increasing and the same loading of LMPB-g-MAH to modified nano-SiO₂ particles, the average diameter of nano-SiO₂ particles decreases gradually, but after GD% of LMPB-g-MAH exceeds 13%, the average diameter increases again. This is because when maleic anhydride groups in every macromolecule chain of LMPB-g-MAH are insufficient, the uncoated nano-SiO₂ will be likely to agglomerate together. While if maleic anhydride groups were superabundant, the modified nano-SiO₂ maybe agglomerate again, because one macromolecular chain maybe modify many nano-particles.

Fig. 8 shows, with the increasing loading and the same GD% (3[#]) of LMPB-g-MAH, the average diameter of nano-SiO₂ decreases gradually, but after the loading of macromolecular coupling agent exceeds 10%, the average diameter increases again. This may because when the loading of LMPB-g-MAH is insufficient, the uncoated nano-SiO₂ will be likely to agglomerate together. While if the loading is superabundant corresponding to the loading of nano-SiO₂, the modified nano-SiO₂ maybe agglomerate again due to the entanglement between long and flexible chains of LMPB-g-MAH.

3.6. Contact angle and surface free energy

The change of surface hydrophilicity was investigated by contact angle measurements. Surface free energy of native and modified nano-SiO₂ was calculated by corresponding contact angle. Table 4 shows an obvious change of contact angle and surface free energy. After the surface modification, the contact angle increases from 20.48° to 42.12°, suggesting increased surface hydrophobicity. These changes are likely due to the carbon backbone of LMPB-g-MAH which is hydrophobic. The surface free energy of nano-SiO₂ also decreases sharply from 266.86 J m^{–2} to 68.30 J m^{–2}. Thus we can conclude that the nano-SiO₂ modified with LMPB-g-MAH can be dispersed in nonpolar or weak polar polymer materials more easily than native nano-SiO₂ particles.

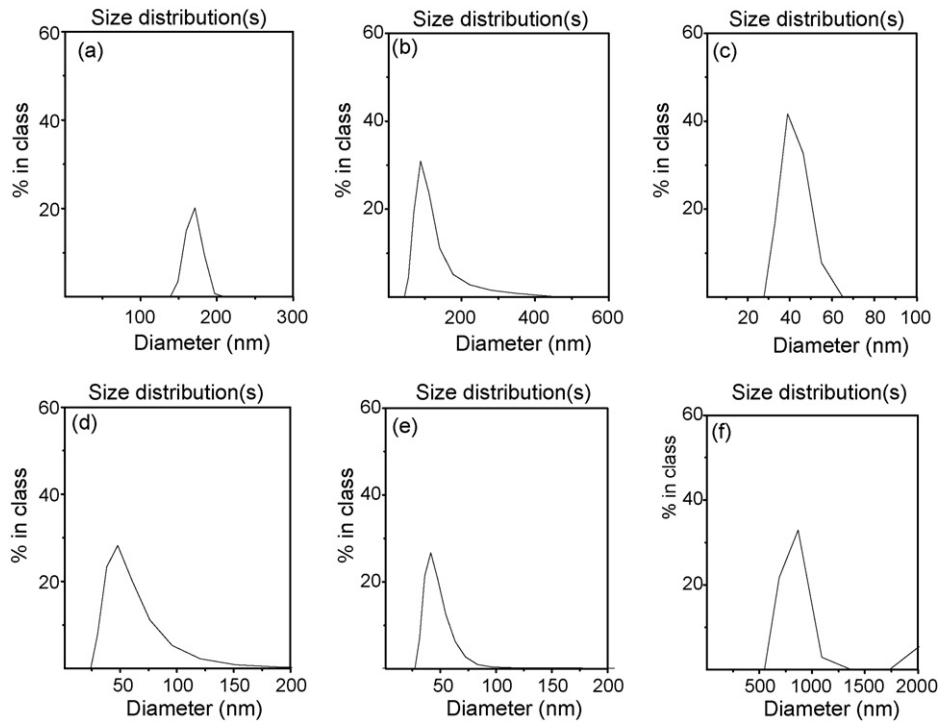


Fig. 7. Size distribution of nano-SiO₂ modified with different percentage macromolecular coupling agent (a) 1[#] (b) 2[#] (c) 3[#] (d) 4[#] (e) 5[#] and (f) unmodified SiO₂.

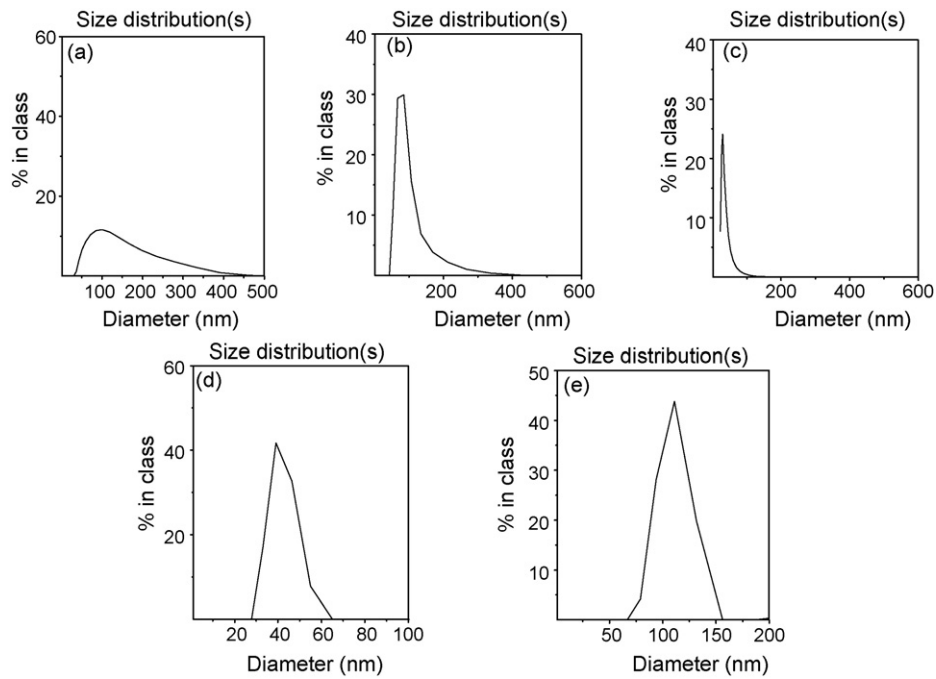


Fig. 8. Size distribution of nano-SiO₂ modified with different percentage macromolecular coupling agent (a) 5% (b) 7% (c) 9% (d) 11% (e) 13%.

Table 4
Contact angle and surface free energy of native and modified nano-SiO₂ at 25 °C

Sample	Contact angle (°)		Surface free energy (J M ⁻²)	γ_D (J m ⁻²)	γ_P (J m ⁻²)
	Water	Glycol			
Native nano-SiO ₂	20.48	57.23	266.86	40.46	226.40
Modified nano-SiO ₂	42.12	25.45	68.30	2.37	65.93

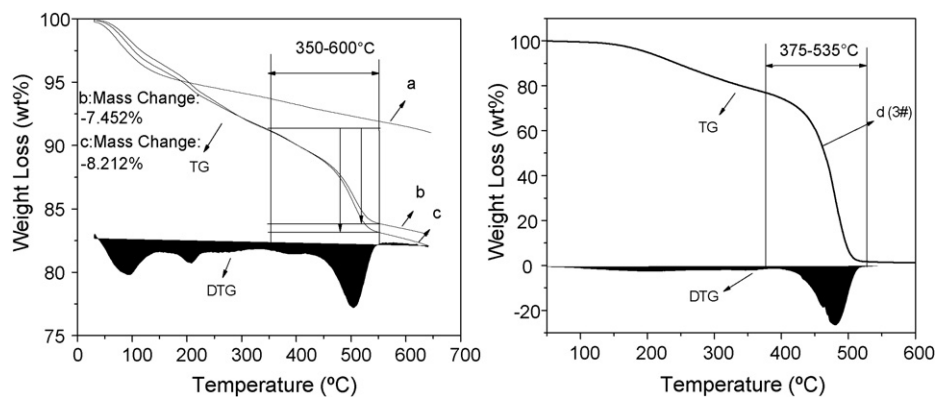


Fig. 9. TGA spectra of (a) modified nano-SiO₂ particles; (b) modified and after extracting modified nano-SiO₂ particles; (c) native nano-SiO₂ particles and (d) LMPB-g-MAH (3#).

3.7. Analysis of TGA

Thermal stability of nano-SiO₂, modified nano-SiO₂ and LMPB-g-MAH was measured by dynamic thermo gravimetric analysis (TGA) as show in Fig. 9 (the heating rate was monitored at 20 °C min⁻¹, and the flow rate of N₂ of 30 ml min⁻¹).

The TGA thermogram of LMPB-g-MAH in nitrogen is shown in Fig. 9(d). The LMPB-g-MAH showed a slight weight loss before 350 °C for its low-molecular weight. A much greater weight loss (78.6 wt%) occurs at the temperature range of 350–625 °C, which is more intuitionistic from the DTG curve.

As shown in Fig. 9(a), the thermal decomposition of native nano-SiO₂ begins at about 60 °C and the continuous mass loss can be seen from 60 °C to 600 °C This is likely due to a series of chemical reactions happening on the surface of nano-SiO₂ between surface groups or some physical and chemical adsorption substances, then the desorption of H₂O, etc. So, native nano-SiO₂'s mass loss is 8.5% at a high decomposition rate in 125–200 °C stage while in 200–600 °C stage the mass loss is only 2.5% at a low decomposition rate.

The modified nano-SiO₂ sample was analyzed before and after being washed with dimethylbenzene in Soxhlet extractor for 72 h. The thermal degradation curves of nano-SiO₂ modified with LMPB-g-MAH are shown in Fig. 9(b) and (c). We can find that both curves are similar with Fig. 9(a) before 350 °C which is assigned to the loss of nano-SiO₂. According to Fig. 9(d), the weight loss from 350 °C to 600 °C is attributed to the degradation of LMPB-g-MAH. In contrast with curve a, curve b shows less weight loss (7.452%) from 350 °C to 600 °C than that of sample c (8.212%). This indicates that the excess LMPB-g-MAH in the sample which cannot bond on the surface of nano-SiO₂ has been extracted by Soxhlet extractor. So we can get the using efficiency, chemical using efficiency, physical using efficiency of the macromolecular LMPB-g-MAH, which are calculated by formular1 as following:

(1). Using efficiency of the micromolecule couple agent

$$(\text{LMPB-g-MAH}) = \frac{8.212\%}{11\%} \times 100 = 74.66\%$$

(2). Chemical using efficiency of the micromolecule couple agent

$$(\text{LMPB-g-MAH}) = \frac{7.452\%}{11\%} \times 100 = 68.29\%$$

(3). Physical using efficiency of the micromolecule couple agent

$$(\text{LMPB-g-MAH}) = \frac{8.212\% - 7.452\%}{11\%} \times 100 = 6.37\%$$

Therefore, it further illustrates that the LMPB-g-MAH macromolecular chains are anchored or grafted on the surface of nano-SiO₂. Otherwise, the LMPB-g-MAH macromolecule should be removed during the curve b.

4. Conclusions

Nano-SiO₂ particles were modified by macromolecular coupling agent (LMPB-g-MAH), which was designed and synthesized by grafting maleic anhydride onto low-molecular-weight polybutadiene liquid rubber in dimethylbenzene using benzoyl peroxide. Study results show that LMPB-g-MAH has been anchored on the surface of nano-SiO₂ particles, the modified nano-SiO₂ particles presented a more stable colloidal dispersion in dimethylbenzene than that of untreated nano-SiO₂, and the using efficiency of LMPB-g-MAH was 74.66%.

Acknowledgments

This research was supported by National Key Technoledges R & D Program (2007BAE22B02), Natural Science Foundation of Anhui Province (050440906), Natural Science Foundation of Educational Office of Anhui Province (Kj2007A044).

References

- [1] Xingwei Li, Gengchao Wang, Xiaoxuan Li, Surface modification of nano-SiO₂ particles using polyaniline, *Surf. Coat. Tech.* 197 (2005) 56–60.
- [2] Young-Woo Ok, Tae-Yeon Seong, Donghwan Kim, et al., Electrical and optical properties of point-contacted a-Si:H/c-Si heterojunction solar cells with patterned SiO₂ at the interface, *Sol. Energ. Mat. Sol. C* 91 (2007) 1366–1370.
- [3] Hongsheng Zhao, Tongxiang Liang, Bing Liu, Synthesis and properties of copper conductive adhesives modified by SiO₂ nanoparticles, *Int. J. Adhes. Adhes.* 27 (2007) 429–433.
- [4] W.M. Tsang, V. Stolojan, B.J. Sealy, et al., Silva Electron field emission properties of Co quantum dots in SiO₂ matrix synthesized by ion implantation, *Ultramicroscopy* 107 (2007) 819–824.
- [5] B. Canut, M.G. Bianchin, V. Teodorescu, et al., Structure of Ni/SiO₂ films prepared by sol-gel dip coating, *J. Non-Cryst. Solids* 353 (2007) 2646–2653.
- [6] M.L. Zhang, G.L. Ding, X.Y. Jing, X.Q. Hou, Preparation, modification and application of nanoscale SiO₂, *Appl. Surf. Tech.* 31 (2004) 64–66.
- [7] Qing-Li Zhang, Lu-Chao Du, Yu-Xiang Weng, Particle-size-dependent distribution of carboxylate adsorption sites on tio₂ nanoparticle surfaces: insights into the surface modification of nanostructured TiO₂ electrodes, *Phys. Chem. B* 108 (2004) 15077–15083.
- [8] A.D. Pomogailo, Synthesis and intercalation chemistry of hybrid organo-inorganic nanocomposites, *Poly. S. Seri. C* 48 (2006) 85–111.
- [9] Faouzi Nsib, Naceur Ayed, Yves Chevalier, Selection of dispersants for the dispersion of carbon black in organic medium, *Prog. Org. Coat.* 55 (2006) 303–310.
- [10] Beata Sweryda-Krawiec, Thierry Cassagneau, Janos H. Fendler, Surface modification of silicon nanocrystallites by alcohols, *J. Phys. Chem. B* 103 (1999) 9524–9529.
- [11] Xuegeng Li, Yuanqing He, Mark T. Swihart, Surface functionalization of silicon nanoparticles produced by laser-driven pyrolysis of silane followed by HF-HNO₃ etching, *Langmuir* 20 (2004) 4720–4727.
- [12] Hua S Fengjun, Mark T. Swihart, Eli Ruckenstein, Efficient surface grafting of luminescent silicon quantum dots by photoinitiated hydrosilylation, *Langmuir* 21 (2005) 6054–6062.
- [13] Abraham Ulman, Formation and structure of self-assembled monolayers, *Chem. Rev.* 96 (1996) 1533–1554.

- [14] F.J. Xu, Q.J. Cai, E.T. Kang, K.G. Neoh, Covalent. Graft polymerization and block copolymerization initiated by the chlorinated $\text{SiO}_2(\text{SiO}_2\text{-Cl})$ moieties of glass and oriented single crystal silicon surfaces, *Macromolecules* 38 (2005) 1051–1054.
- [15] Ru Xia, Yuchuan Zhang, Qingren Zhu, et al., Surface modification of nano-sized silicon nitride with BA-MAA-AN tercopolymer, *J. Appl. Polym. Sci.* 107 (2008) 562–570.
- [16] Ru Xia, Minghua Li, Yuchuan Zhang, et al., Synthesis of tercopolymer BA-MMA-VTES and surface modification of nano-size Si_3N_4 with this macromolecular coupling agent, *J. Appl. Polym. Sci.* 107 (2008) 1100–1107.
- [17] Xia Ru, Zhang Yuchuan, Zhu Qingren, Study on nano- Si_3N_4 /NBR composites' properties, in: *Proceeding of 5th National (Int.) nanoscience tech.*, Xi'an, 11, 2006, pp. 554–560 (in Chinese).
- [18] Jun-Feng Su, Li-Xin Wang, Li Ren, Synthesis of polyurethane microPCMs containing *n*-octadecane by interfacial polycondensation: influence of styrene-maleic anhydride as a surfactant, *Colloid Surf. A* 299 (2007) 268–275.
- [19] Sonia Marli Bohrz Nachtigall, Macromolecular coupling agents for flame retardant materials, *Eur. Polym. J.* 42 (2006) 990–999.
- [20] Chahira Makhlof, Steiphane Marais, Sadok Roudesli, Graft copolymerization of acrylic acid onto polyamide fibers., *Appl. Surf. Sci.* 253 (2007) 5521–5528.
- [21] Dabid D. Jiang, Charles A. Wilkie, Graft copolymerization of methacrylic acid acrylic acid and methyl crylate onto styrene-butadiene block copolymer, *Eur. Polym. J.* 34 (1998) 997–1006.
- [22] Tao Sun, Peixin Xu, Qing Liu, et al., Graft copolymerization of methacrylic acid onto carboxymethyl chitosan, *Eur. Polym. J.* 39 (2003) 189–192.
- [23] Hongbo Ni, Study on grafting of maleic anhydride onto low relative molecular mass *trans*-1,4-polybutadiene, *China Elas.* 14 (2004) 11–15.
- [24] David Carrie're, Meilanie Moreau, Philippe Barboux, et al., Modification of the surface properties of porous nanometric zirconia particles by covalent grafting, *Langmuir* 20 (2004) 3449–3455.
- [25] Erjun Tang, Guoxiang Cheng, Xiaolu Ma, et al., Surface modification of zinc oxide nanoparticles by PMAA and its dispersion in aqueous system, *Appl. Surf. Sci.* 252 (2006) 5227–5232.
- [26] Jianfei Che, Baoyong Luan, Xujie Yang, Graft polymerization onto nano-sized SiO_2 surface and its application to the modification of PBT, *Mater. Lett.* 59 (2005) 1603–1609.
- [27] Jing Peng, Haibing Xia, Maolin Zhai, Radiation-induced graft polymerization of maleic acid and maleic anhydride onto ultra-fine powdered styrene-butadiene rubber (UFSB), *Radiat. Phys. Chem.* 76 (2007) 1741–1745.
- [28] Wulin Qiu, Takashi Endo, Takahiro Hirotsu, A novel technique for preparing of maleic anhydride grafted polyolefins, *Eur. Polym. J.* 41 (2005) 1979–1984.
- [29] Qingchun Zhao, Wenming Chen, Qingren Zhu, Self-assembly and characterization of novel amorphous $\text{SiO}_x(x=21)$ nanospheres, *Nanotechnology* 15 (2004) 958–961.
- [30] Matthias Beinhoff, Jane Frommer, Kenneth R. Carter, Photochemical attachment of reactive cross-linked polymer films to Si/ SiO_2 surfaces and subsequent polymer brush growth, *Chem. Mater.* 18 (2006) 3425–3431.
- [31] A. Kohut, A. Voronov, W. Peukert, An effective way to stabilize colloidal particles dispersed in polar and nonpolar media, *Langmuir* 23 (2007) 504–508.